Mel-18 Negatively Regulates *INK4a/ARF*-Independent Cell Cycle Progression via Akt Inactivation in Breast Cancer

Jeong-Yeon Lee,[1] Ki-Seok Jang,[1] Dong-Hui Shin,[1] Mi-Yun Oh,[1] Hyun-Jun Kim,[1] Yongseok Kim,[2] and Gu Kong[1]

Departments of [1]Pathology and [2]Biochemistry, College of Medicine, Hanyang University, Seoul, Republic of Korea

Abstract

Mel-18, a polycomb group (PcG) protein, has been suggested as a tumor suppressor in human breast cancer. Previously, we reported that Mel-18 has antiproliferative activity in breast cancer cells. However, its functional mechanism has not been fully elucidated. Here, we investigated the role of Mel-18 in human breast cancer. We saw an inverse correlation between Mel-18 and phospho-Akt, which were expressed at low and high levels, respectively, in primary breast tumor tissues from 40 breast cancer patients. The effect of Mel-18 on cell growth was examined in two breast cancer cell lines, SK-BR-3 and T-47D, which express relatively low and high levels of endogenous Mel-18, respectively. On Mel-18 overexpression in SK-BR-3 cells, cell growth was attenuated and G_1 arrest was observed. Likewise, suppression of Mel-18 by antisense expression in T-47D cells led to enhanced cell growth and accelerated G_1-S phase transition. In these cells, cyclin-dependent kinase (Cdk)-4 and Cdk2 activities were affected by Mel-18, which were mediated by changes in cyclin D1 expression and $p27^{Kip1}$ phosphorylation at Thr^{157}, but not by *INK4a/ARF* genes. The changes were both dependent on the phosphatidylinositol 3-kinase/Akt signaling pathway. Akt phosphorylation at Ser^{473} was reduced by Mel-18 overexpression in SK-BR-3 cells and enhanced by Mel-18 suppression in T-47D cells. Akt-mediated cytoplasmic localization of $p27^{Kip1}$ was inhibited by Mel-18 in SK-BR-3 cells. Moreover, Mel-18 overexpression showed reduced glycogen synthase kinase-3β phosphorylation, β-catenin nuclear localization, T-cell factor/lymphoid enhancer factor promoter activity, and cyclin D1 mRNA level. Taken together, we established a linear relationship between Mel-18→Akt→G_1 phase regulators. [Cancer Res 2008;68(11):4201–9]

Introduction

Polycomb group (PcG) proteins are highly conserved factors that act as transcriptional repressors. They were originally identified in *Drosophila* and play a crucial role in maintaining repression of homeotic genes during development (1). PcG proteins control many diverse biological processes, including cellular differentiation, proliferation, and tumorigenesis (2, 3). They form multimeric protein complexes and epigenetically regulate many target genes through chromatin modification (2). These proteins are classified into two distinct groups: one is the polycomb repressive complex 2 group, which is thought to initiate repression by methylating histone H3 lysine 9 and 27, and another is the polycomb repressive complex 1 group, which is considered to be involved in maintenance of repression (2, 3).

Mel-18, also known as polycomb group ring finger protein, is a constituent of polycomb repressive complex 1. Mel-18 is highly homologous to Bmi-1 by sharing 57% amino acid identity and a zinc finger named RING at its NH_2 terminus. Wiederschain et al. (4) have recently reported that Bmi-1 and Mel-18 in HeLa cells compose nearly identical core proteins by sharing many constituents, such as Ring1, Ring2, RYBP, HPH1, HPH2, HPH3, CBX4, and CBX8. Despite their structural similarities, many studies report differences in their roles in cancer cell growth and survival. Unlike Bmi-1, which is overexpressed in various human tumors and generally accepted as a proto-oncogene (4–7), Mel-18 is shown to be either oncogenic or tumor suppressive, depending on the cancer system. Mel-18 was originally cloned from B16 mouse melanoma cells and their transcripts were shown to be highly expressed in many tumor cells including human melanoma and Hodgkin's lymphomas (8, 9). Mel-18 and Bmi-1 are highly expressed in DAOY medulloblastoma cells and small hairpin RNA–mediated knockdown of either one or both of them in DAOY cells inhibits cancer cell growth *in vitro* and suppresses the growth of human medulloblastoma xenografts *in vivo* (4). However, markedly enhanced tumorigenicity has been shown in nude mice injected with NIH 3T3 cells overexpressing antisense *mel-18*, but not with sense construct (10). We have also reported that Mel-18 directly interacts with cyclin D2 and knockdown of Mel-18 by antisense construct in T-47D breast cancer cells enhances cell proliferation (11). Recently, Guo et al. (12) reported an inverse correlation between Mel-18 and Bmi-1 expression in breast cancer cell lines and primary human breast tumors. Furthermore, they have shown Mel-18 as a tumor suppressor in MCF7 breast cancer cells and suggested repression of Bmi-1 expression and down-regulation of Akt activity as its mechanism. Therefore, the functional role of Mel-18 should be carefully interpreted within the context of a cancer system.

Akt signaling plays a crucial role in many biological processes including cell proliferation and survival. Its aberrant activation contributes to tumor progression in many types of human cancer including breast cancer (13). Akt promotes cell proliferation through its many downstream effectors. Particularly, Akt positively regulates G_1 to S transition in cell cycle progression through regulation of D-type cyclins and cyclin-dependent kinase (Cdk) inhibitors, such as $p27^{Kip1}$, at the transcriptional level. Akt controls the canonical Wnt pathway (14, 15). Akt-dependent phosphorylation of the Forkhead family transcription factors leads to their nuclear exclusion and, thus, inhibition of FoxO factor–mediated gene expression including $p27^{Kip1}$ (16, 17) and up-regulation of cyclin D1 (18). Moreover, Akt regulates the stability and subcellular localization of G_1 regulators. Akt-dependent inactivation of glycogen synthase kinase-3β (GSK-3β) blocks cyclin D1 phosphorylation

Requests for reprints: Gu Kong, Department of Pathology, College of Medicine, Hanyang University, 17 Haengdang-dong, Seongdong-gu, Seoul, 133-791, Republic of Korea. Phone: 82-2-2290-8251; Fax: 82-2-2295-1091; E-mail: gkong@hanyang.ac.kr.

doi:10.1158/0008-5472.CAN-07-2570

at Thr^{286}, which protects cyclin D1 from proteolytic degradation (19). Phosphorylation of $p27^{Kip1}$ at Thr^{157} by Akt causes cytoplasmic retention, which blocks binding to nuclear Cdk2/cyclin E (20–22). Similarly, $p21^{Cip1/WAF1}$ is retained in the cytoplasm on phosphorylation at Thr^{145} by Akt (23).

Previously, we have reported that loss of Mel-18 expression accelerates cell proliferation of T-47D human breast cancer cells (11). However, its exact mechanism remains undefined. To elucidate the growth regulatory mechanism of Mel-18, we investigated the effect of Mel-18 on cell cycle in breast cancer cells. In this study, we found that Mel-18 attenuated cell growth and caused G_1 arrest by down-regulation of cyclin D1 expression and $p27^{Kip1}$ phosphorylation at Thr^{157} via inactivation of the Akt signaling pathway. Our data suggest that Mel-18 controls cell cycle as a negative regulator of Akt and may have a possibility of being the tumor suppressor gene in human breast cancer.

Materials and Methods

Tissue samples from patients. Fresh frozen normal and tumor tissues were obtained from 40 patients of invasive ductal carcinoma who underwent surgery between 2002 and 2005 at Hanyang University Hospital (Seoul, Korea).

Cell lines, kinase inhibitors, and antibodies. T-47D cells were maintained in RPMI 1640 (Welgene) supplemented with 10% fetal bovine serum (FBS; Welgene) and SK-BR-3 cells were maintained in DMEM (Welgene) containing 10% FBS at 37°C in a humidified 5% CO_2 incubator. The phosphatidylinositol 3-kinase inhibitor LY294002 and the mitogen-activated protein kinase (MAPK)/extracellular signal-regulated kinase (Erk) kinase (MEK) inhibitor PD98059 were from Sigma. For immunoblottings and immunoprecipitations, the following antibodies were used: antibodies against Akt, Ser^{473} phospho-Akt, GSK-3β, Ser^{9} phospho-GSK-3β, phospho-MAPK, and $p15^{INK4b}$ (Cell Signaling Technology); cyclin D1, cyclin E, $p27^{Kip1}$, Cdk2, Cdk4, Cdk6, Mel-18, Bmi-1, and Sp1 (Santa Cruz Biotechnologies); Thr^{157} phospho-$p27^{Kip1}$ (R&D Systems); total MAPK (Erk42/44; Zymed Laboratories); total β-catenin (Upstate Biotechnology); α-tubulin (Calbiochem); $p27^{Kip1}$ and β-catenin (BD Transduction Laboratories); Cy5-conjugated antimouse IgG (Jackson Immunoresearch); and β-actin and phycoerythrin-conjugated antirabbit IgG (Sigma).

Plasmids, transfection, and retroviral infection. Full-length Mel-18 cDNA in pOTB7 vector was purchased (clone MGC-10336; American Type Culture Collection). The retroviral vector pCL-IRES3-EGFP was a generous gift from Chang-Hwan Park (Hanyang University, Seoul, Korea). The $p27^{Kip1}$ΔNLS mutant construct (24) was kindly provided by Incheol Shin (Hanyang University, Seoul, Korea). Mel-18 cDNA in pOTB7 was cut with *Bam*HI and *Xho*I restriction enzymes, blunt-ended with Klenow, and subcloned into *Xho*I-cut and blunt-ended pCL-IRES3-EGFP vector. Subcloned Mel-18 cDNA clones in the forward and reverse orientations were used as expression and antisense constructs, respectively. H29D cells were transfected with each plasmid using Lipofectamine (Invitrogen). After 48-h transfection, the medium containing retroviruses was harvested, filtered through 0.45-μm filters, and transferred to target cells with 6 μg/mL polybrene (Sigma) or stored in aliquots at −70°C for later use. The infected cells were transiently used in experiments or selected with 10 μg/mL blasticidin S (Invitrogen) for 6 d, maintained with the medium containing 2 μg/mL blasticidin S, and used as stable cells.

Cell proliferation assay. The CellTiter 96 nonradioactive cell proliferation assay kit (Promega) was used for measurement of cell proliferation. As described by the manufacturer, cells were seeded onto 96-well plates and incubated with 3-[4,5-dimethylthiazol-2-yl]-2,5-diphenyltetrazolium bromide (MTT) dye solution at 37°C for 4 h, and stopped by addition of solubilization/stop solution. The formazan product was measured at 570-nm absorbance using a microplate reader (Bio-Rad).

Cell cycle analysis. Cells were trypsinized, washed once with ice-cold PBS, and fixed with 75% ethanol at −20°C for 2 h. After washing twice with PBS, cells were stained with 10 μg/mL propidium iodide (Sigma) containing 1 mg/mL RNase at 37°C for 20 min in the dark and analyzed with FACSCalibur flow cytometer and CellQuest software (BD Biosciences).

Reverse transcription-PCR. Total RNA was isolated with Trizol (Invitrogen) and reverse transcription-PCR (RT-PCR) was done with Access RT-PCR system (Promega) according to the instructions of the manufacturers. The cDNA amplification was carried out using the GeneAmp PCR system (Perkin-Elmer) as follows: 94°C for 5 min, 22 to 28 cycles of 94°C for 1 min, 54°C to 58°C for 1 min, 72°C for 1.5 min, and 72°C for 10 min. The following specific primers were used for PCR reaction: cyclin D1, 5′-AGCCATGGAACACCAGCTC-3′ and 5′-GCACCTCCAGCATCCAGGT-3′; cyclin E, 5′-ATACAGACCCACAGAGACAG-3′ and 5′-TGCCATCCACAGAAATACTT-3′; $p27^{Kip1}$, 5′-CAAACGTGCGAGTGTCTAACG-3′ and 5′-GCAGGTCGCTTCCTTATTCCT-3′; $p15^{INK4b}$, 5′-GGTAAGAAAATAAAGTCGTT-3′ and 5′-GGAATGCGCGAGGAGAACAA-3′; mel-18, 5′-GTACTTCATCGACGCCACCACTATC-3′ and 5′-CTCGTCCTCGTACAGAACCTCCA-3′; and β-actin, 5′-CCAGAGCAAGAGAGGTATCC-3′ and 5′-CTGTGGTGGTGAAGCTGTAG-3′.

Immunoblotting and immunoprecipitation. Cells were lysed in radioimmunoprecipitation assay (RIPA) buffer and immunoblotting was carried out as described (25). For immunoprecipitation, 1 μg of Cdk4 and Cdk2 antibodies was chemically cross-linked with 20 mmol/L dimethyl pimelimidate (Sigma) in 0.2 mol/L sodium tetraborate (pH 9.0) to 20 μL of protein A agarose (Upstate Biotechnology). Cell lysates (1 mg) and the cross-linked antibodies were immunoprecipitated as described (25).

***In vitro* kinase assay.** Total cell lysates were immunoprecipitated with anti-Cdk4 or anti-Cdk2 antibodies at 4°C for 16 h. The immunoprecipitant was washed thrice with RIPA buffer, once with kinase buffer [50 mmol/L Tris (pH 7.5), 10 mmol/L $MgCl_2$, 2.5 mmol/L EGTA, 1 mmol/L DTT], and reacted in kinase buffer containing 20 μmol/L of ATP, 10 μCi of [γ-^{32}P]ATP (6,000 Ci/mmol; Amersham Life Science), and 5 μg of histone H1 (Sigma), a Cdk2 substrate, or 2 μg of glutathione *S*-transferase-pRb (Santa Cruz Biotechnologies), a Cdk4 substrate, at 30°C for 30 min. The reaction was stopped by adding 10 μL of 5× SDS sample buffer, and the mixture was heated at 95°C for 5 min. The radioactive kinase activity was visualized by SDS-PAGE (15% gel) and autoradiography.

Cell fractionation. Cell fractionation was carried out using NE-PER Nuclear and cytoplasmic extraction reagents (Pierce) as described by the manufacturer. Briefly, 2×10^6 cells were pelleted and lysed in 200 μL of ice-cold CER I buffer and 11 μL of ice-cold CER II buffer. After centrifugation at 4°C for 5 min, the supernatant (cytoplasmic extract) was collected and the pellet was resuspended in 50 μL of ice-cold NER buffer and vortexed for 15 s every 10 min, for a total of 50 min. After centrifugation at 4°C for 10 min, the supernatant was collected as nuclear extract. The extracts were subjected to immunoblotting or stored at −80°C until use.

Immunofluorescence staining. Cells (1×10^5 per chamber) were seeded onto a four-chamber slide glass (Lab-Tek II Chamber Slide System, Nalge Nunc International) for 16 h, washed with PBS, fixed with 4% paraformaldehyde for 30 min, and permeabilized with 0.2% Triton X-100 for 5 min. After blocking with 3% bovine serum albumin for 1 h, cells were stained with appropriate primary antibodies diluted 1:200 at 4°C for 16 h. Phycoerythrin-conjugated antirabbit IgG (1:200) and Cy5-conjugated antimouse IgG (1:200) were used as secondary antibodies. To visualize the nucleus, 4′6-diamidino-2-phenylindole (DAPI) staining was also done as previously described (26). Immunofluorescence was detected by fluorescence microscopy (Nikon).

Reporter assay. Cells were seeded at 1×10^5 per well in a 12-well plate, and then transfected with 1 μg of pTOP-FLASH, a T-cell factor/lymphoid enhancer factor (TCF/LEF) promoter, or pFOP-FLASH, a TOP mutant form (27), and β-gal cDNAs using FuGENE6 reagent (Roche Diagnostics Corp.). After incubation for 24 h, the cells were infected with retrovirus encoding empty vector or Mel-18 for 48 h. Luciferase activity, expressed as relative light units, was measured using Luciferase Assay system (Promega) and MicroLumat Plus LB96V luminometer (Berthold Technologies) and normalized by β-galactosidase activity.

Statistical analysis. The Western blot and RT-PCR band densities were determined using AlphaEase FC Software (AlphaInnotech, Inc.) and statistical analysis was done with Fisher's exact test or Student's *t* test using SPSS software (SPSS version 11.0).

Results

Loss of Mel-18 correlates with phosphorylated Akt in primary human breast cancer. Increased Akt activity plays a key role in cancer progression and it is frequently activated in various human cancers including breast cancer (28). To investigate whether Mel-18 expression and Akt activity have correlation in human primary breast cancer, we tested Mel-18 expression and Akt phosphorylation at Ser^{473}, a recognition site for Akt activation, in pairs of normal and tumor breast tissues from individual breast cancer patients by immunoblotting. Mel-18 was expressed in both normal and tumor tissues. However, 32 of 40 tumors showed significantly reduced Mel-18 expression compared with normal tissues (Fig. 1, *top*). Furthermore, we found that the tumor cells, which have lower expression of Mel-18 compared with normal tissue, showed enhanced Akt phosphorylation (Fig. 1, *bottom*). Akt phosphorylation was increased in 24 of 40 tumor tissues but total Akt expression remained unchanged. Our result shows an inverse correlation between Mel-18 and Akt activity in human clinical samples, suggesting that loss of Mel-18 may play an important role in breast cancer progression.

Mel-18 attenuates cell growth by G_1 arrest in human breast cancer. To examine the role of Mel-18 in human breast cancer cells, we first measured Mel-18 protein and mRNA levels in various human breast cancer cell lines by Western blot analysis and RT-PCR, respectively. In estrogen receptor–positive T-47D and MCF7 cell lines, Mel-18 was moderately or highly expressed, whereas in estrogen receptor–negative SK-BR-3, MDA-MB-231, and MDA-MB-435 cell lines, low expression was seen (Fig. 2*A*). Next, the role of Mel-18 in breast cancer cell proliferation was examined in two breast cancer cell lines, SK-BR-3 and T-47D cells, where endogenous Mel-18 expression levels are low and high, respectively. To overexpress or suppress Mel-18 expression in low- or high-expressing cells, we generated retroviral Mel-18 and Mel-18 antisense constructs, respectively. SK-BR-3 cells, which have low expression of Mel-18, were infected with retrovirus encoding Mel-18 cDNA and selected with blasticidin S. Mel-18 overexpression in the stable cells was confirmed by Western blot analysis (Fig. 2*B, top left*) and the effect of Mel-18 on cell growth was determined by MTT assay. There was an inverse relationship between Bmi-1 and Mel-18 on Mel-18 overexpression or suppression (Fig. 2*B*), which is consistent with a previous report (12). As shown in Fig. 2*B* (*bottom left*), cell growth was attenuated in Mel-18–overexpressing SK-BR-3 cell lines ($P < 0.05$, Student's t test). Because of the difficulty in long-term maintenance of the stable cells, attributed to the growth inhibitory effect of Mel-18, and comparable efficiency in Mel-18 transduction, all further experiments in this article were done after transient retroviral transduction. SK-BR-3 cells were retrovirally infected with Mel-18 for 24 hours and cell cycle was analyzed by flow cytometry after 72 hours. As seen in Fig. 2*B* (*right*), the percentage of G_1 phase cells was increased and S phase was slightly reduced in the Mel-18–overexpressing cells ($P < 0.05$, Student's t test). Furthermore, we blocked Mel-18 expression in T-47D cells using a retrovirus encoding a Mel-18 antisense construct. As shown in Fig. 2*C*, Mel-18 expression was effectively suppressed by the Mel-18 antisense construct as assessed by Western blot analysis (*top left*). In nonsynchronized cells, cell growth was not affected by expression of Mel-18 antisense (data not shown). However, when cells were restimulated with 10% FBS after serum starvation for 48 hours, cell growth was enhanced and the proportion of S phase cells was increased by antisense construct–mediated knockdown of Mel-18 expression as assessed by MTT assay (Fig. 2*C, bottom left*) and cell cycle analysis, respectively (Fig. 2*C, right*; $P < 0.05$, Student's t test). Taken together, these results indicate that Mel-18 attenuates growth of breast cancer cells through G_1 arrest.

Mel-18–mediated G_1 arrest occurs by down-regulation of Cdk4 and Cdk2 activities via changes in cyclin D1, cyclin E, and $p27^{Kip1}$, but not *INK4a/ARF* family genes. Because we observed changes in G_1 to S transition by Mel-18 overexpression or suppression (Fig. 2), we examined whether Mel-18 affected Cdk4 and Cdk2 activities. In Mel-18–overexpressing SK-BR-3 cells, Cdk4 kinase activity was decreased whereas Cdk2 kinase activity was not changed ($P = 0.001$, Student's t test; Fig. 3*A, left*). On knockdown of Mel-18 expression in T-47D cells, both Cdk4 and Cdk2 activities were augmented ($P = 0.034$ and $P = 0.038$, respectively, Student's t test; Fig. 3*A, right*). Total amounts of Cdk4 and Cdk2 proteins were unchanged in both cell lines (Fig. 3*A, Input*). We next explored the effect of Mel-18 on the expression of G_1 phase regulators, cyclins and Cdk inhibitors, which could affect Cdk4 and Cdk2 activities. In Mel-18–infected SK-BR-3 cells, cyclin D1 expression was down-regulated whereas cyclin E expression was unchanged

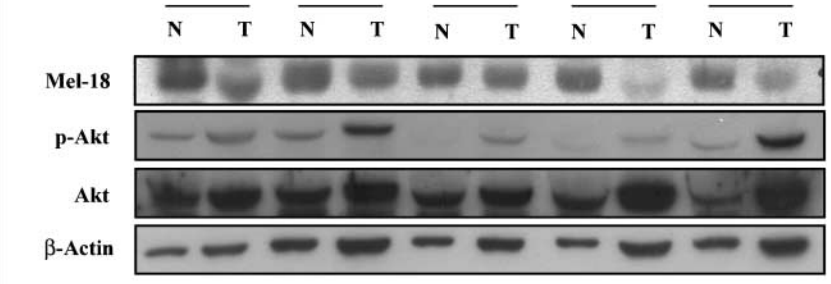

Expression of Mel-18 and phosphorylated Akt in 40 breast cancer patients ($P = 0.042$)

	Mel-18 low (N>T)	Mel-18 high (N≤T)	Total
p-Akt high	22 (55%)	2 (5%)	24 (60%)
p-Akt low	10 (25%)	6 (15%)	16 (40%)
Total	32 (80%)	8 (20%)	40 (100%)

Figure 1. The relationship between Mel-18 expression and Akt phosphorylation at Ser^{473} in human primary breast tumors. Cell lysates (50 μg of protein) of normal breast tissue (*N*) and breast tumor tissue (*T*) pairs from individual breast cancer patients were subjected to immunoblotting with Mel-18, phospho-Akt, and total Akt antibodies (*top*). The densities of the immunoblotting bands were measured, and the expression levels of phospho-Akt in 40 of breast cancer patients who have low Mel-18 expression (normal > tumor) or high expression (normal ≤ tumor) were measured and statistically analyzed with Fisher's exact test (*bottom*).

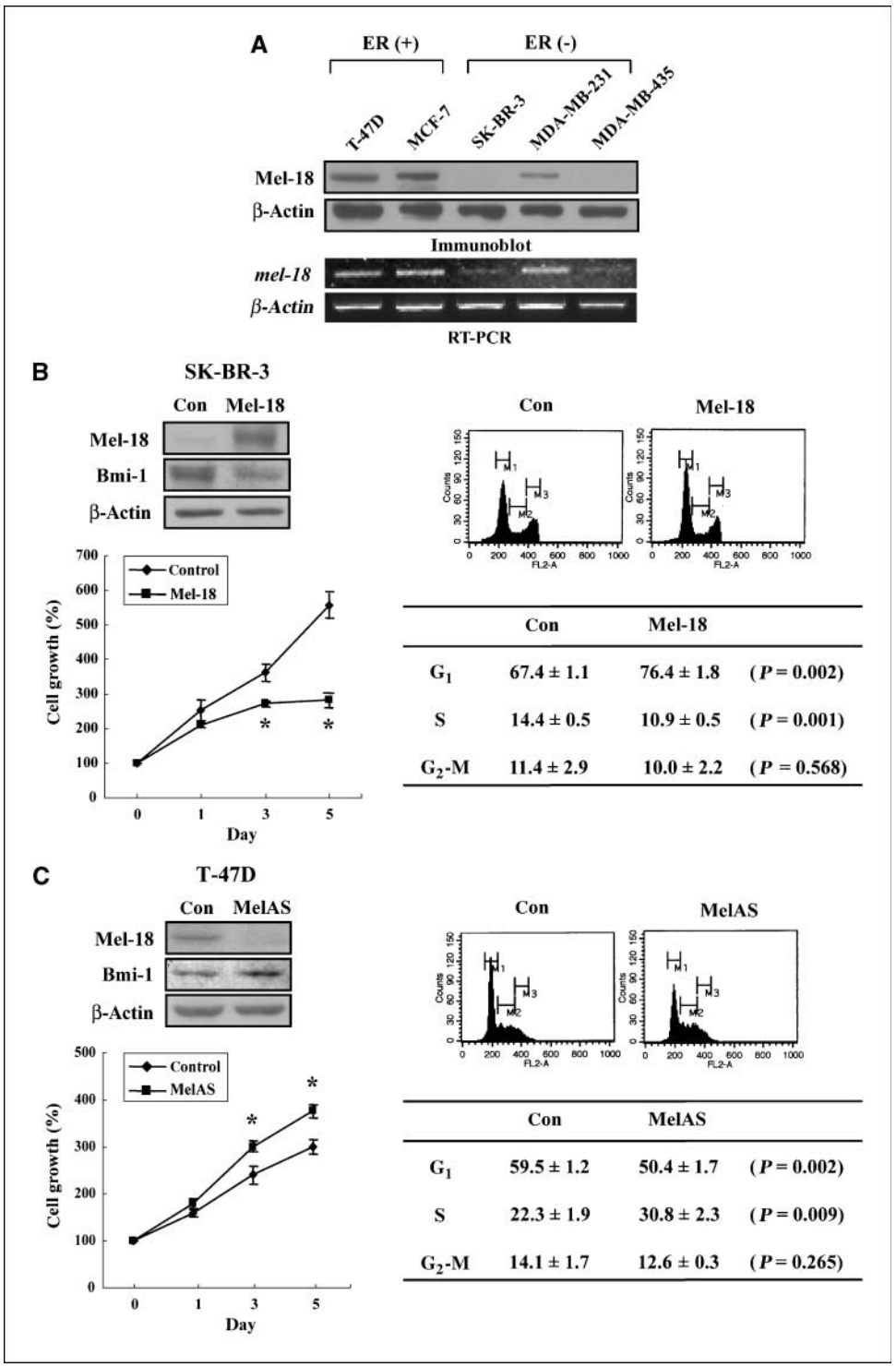

Figure 2. Effect of Mel-18 on cell proliferation and cell cycle in human breast cancer cell lines. *A,* Mel-18 expression was quantified in various breast cancer cell lines. Cell lysates (50 μg) and total RNA of human breast cancer cell lines were subjected to Western blot analysis and RT-PCR, respectively. β-Actin was used as a loading control. *ER,* estrogen receptor. *B,* SK-BR-3 cells were infected with retrovirus encoding empty vector (*Con*) or Mel-18 cDNA (*Mel-18*) and selected with antibiotics as described in Materials and Methods. Two weeks after selection, which is equivalent of 16 d after viral infection, Mel-18 overexpression was confirmed by immunoblotting (*top left*). These cells were serum starved for 24 h for synchronization and subjected to MTT assay for up to 5 d (*bottom left,* day 0 set as time of release with complete medium with 10% FBS). After transient transduction of Mel-18 cDNA by retroviral infection for 24 h, the cell cycle was analyzed by flow cytometry after 72 h and the percentage of each phase (G_1-M) was indicated on the right. *C,* T-47D cells were infected with retrovirus expressing empty vector (*Con*) or Mel-18 antisense construct (*MelAS*). At 24 h posttransduction, cells were serum starved for 48 h, restimulated with 10% FBS–containing medium for 24 h, and then subjected to immunoblotting (*top left*). Identically transduced, starved, and released cells were subjected to MTT assay for up to 5 d (*bottom left*; day 0 set as the time of release with complete medium). Cell cycle analysis was done with cells treated identically as day 5 of MTT assay (*right*). All of data were done in triplicate and statistically analyzed with Student's *t* test. The results are shown as mean ± SD. *, $P < 0.05$.

($P < 0.001$, Student's *t* test; Fig. 3*B, left*). On the other hand, both cyclin D1 and cyclin E expressions were up-regulated by Mel-18 blockade in T-47D cells ($P = 0.002$ and $P = 0.045$, respectively, Student's *t* test; Fig. 3*B, right*). In addition, total amount of $p27^{Kip1}$ remained unchanged, but phosphorylation of $p27^{Kip1}$ at Thr^{157}, which is involved in cytoplasmic localization, was significantly reduced by Mel-18 overexpression in SK-BR-3 cells and enhanced by Mel-18 suppression in T-47D cells ($P < 0.001$ and $P = 0.019$, respectively, Student's *t* test; Fig. 3*B*). Identical expression patterns were seen at the mRNA level when assessed by RT-PCR (cyclin D1 in SK-BR-3, $P = 0.023$; in T-47D, $P = 0.023$, Student's *t* test; Fig. 3*C*). Because Mel-18 is known as a regulator of *INK4a/ARF* family (29–31), we also investigated $p16^{INK4a}$, $p15^{INK4b}$, and $p14^{ARF}$ expressions in these cell lines. Although $p15^{INK4b}$ was expressed in both cell lines, its expression remained unchanged by overexpression or suppression of Mel-18 (Fig. 3*B* and *C*). The protein level of $p16^{INK4a}$ was not detected in both SK-BR-3 and T-47D cells (data not shown). Both protein and mRNA levels of $p14^{ARF}$ were very weak in T-47D

cells and its expression was unchanged in both SK-BR-3 and T-47D cell lines (data not shown). Next, we examined whether the changes seen with total protein were reflected in the association with G_1 phase Cdks. As shown in Fig. 3*D* (*left*), on Mel-18 overexpression in SK-BR-3, the amount of Cdk4-associated cyclin D1 was decreased ($P < 0.001$, Student's t test). Moreover, the amount of Cdk4-associated $p27^{Kip1}$ was decreased whereas Cdk2-associated $p27^{Kip1}$ was increased as determined by coimmunoprecipitaion, suggesting that $p27^{Kip1}$ was shifted from Cdk4 to Cdk2 in Mel-18–overexpressing SK-BR-3 cells ($P < 0.001$ and $P = 0.019$, respectively, Student's t test). The amount of Cdk2-associated cyclin E remained unchanged. In T-47D cells, coimmunoprecipitation showed the increase in the amounts of both Cdk4-associated cyclin D1 and Cdk2-associated cyclin E ($P = 0.023$ and $P = 0.016$,

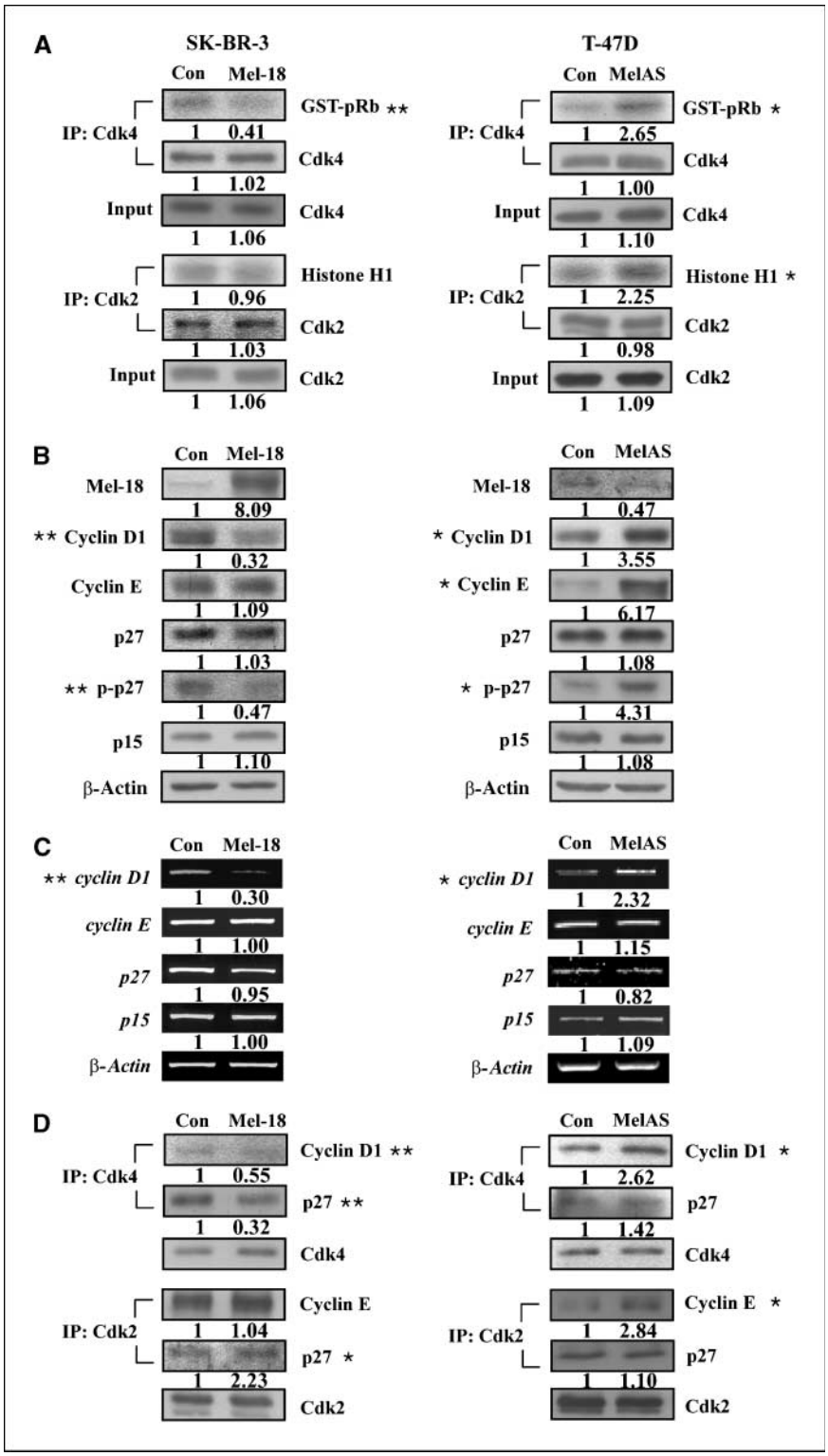

Figure 3. Effect of Mel-18 on G_1 regulators in human breast cancer cell lines. Cell lysates of SK-BR-3 cells, retrovirally transduced to express empty vector (*Con*) or Mel-18, were prepared at 72 h after transient infection for 24 h. Cell lysates of T-47D cells, infected with empty vector (*Con*) or Mel-18 antisense (*Mel AS*), were made 5 d after release from synchronization as in Fig. 2*C*. *A, in vitro* kinase assays of immunoprecipitated Cdks (*IP: Cdk4* and *IP: Cdk2*) from Mel-18–overexpressing SK-BR-3 cells (*left*) and Mel-18–suppressed T-47D cells (*right*) were done with appropriate substrates as indicated. *Input*, immunoblots of whole-cell lysates with antibodies indicated on the right. *GST,* glutathione *S*-transferase. *B* and *C,* transiently transduced SK-BR-3 and T-47D were subjected to immunoblotting and RT-PCR to examine the expressions of G_1 regulators. *D,* the identical cell lysates in *A* were immunoprecipitated with anti-Cdk2 or Cdk4 antibody and the amounts of associated cyclin D1, cyclin E, and $p27^{Kip1}$ were quantified by immunoblotting. Representative of three independent experiments with similar results. Each blot density was quantified. * and **, $P < 0.05$, statistically significant increase and decrease, respectively (Student's t test).

respectively, Student's *t* test; Fig. 3*D, right*). The amounts of both Cdk2- and Cdk4-associated $p27^{Kip1}$ were unchanged (Fig. 3*D, right*). Therefore, these results indicate that Mel-18–mediated G_1 arrest is attributed to changes in G_1 cyclin expression and $p27^{Kip1}$ phosphorylation, but not in *INK4a/ARF* expressions, in human breast cancer cell lines.

Mel-18–induced G_1 arrest is mediated by the Akt signaling pathway. To understand the molecular mechanism involved in the Mel-18–mediated regulation of cyclin D1 expression and $p27^{Kip1}$ phosphorylation, we investigated the upstream signaling pathways of cell cycle regulators. Because we saw an inverse correlation between Mel-18 and Akt phosphorylation in primary breast cancer (Fig. 1) and both cyclin D1 expression and $p27^{Kip1}$ phosphorylation at Thr^{157} can be regulated by Akt (32), we investigated the Akt signaling pathways in Mel-18– or Mel-18 antisense–infected breast cancer cell lines. In SK-BR-3 cells, Akt phosphorylation at Ser^{473}, a recognition site for Akt activation, was significantly diminished by Mel-18 overexpression as assessed by immunoblotting ($P < 0.001$, Student's *t* test; Fig. 4*A*). Consistent with these results, knockdown of Mel-18 expression augmented Akt phosphorylation at Ser^{473} ($P = 0.001$, Student's *t* test; Fig. 4*B*). Total amount of Akt was unchanged in both cells. Because cyclin D1 expression can also be regulated by the MAPK signaling pathway (33), we also investigated this pathway in Mel-18– or Mel-18 antisense–transduced breast cancer cell lines. Phosphorylation and total amount of Erk1/2 were unchanged in both cell lines (Fig. 4*A* and *B*). To confirm that the changes of cell cycle regulators were Akt-dependent effects in Mel-18 antisense–infected T-47D cells, we treated the cells with 40 μmol/L of LY294002, a phosphatidylinositol 3-kinase inhibitor, and/or 50 μmol/L of PD98059, a MEK inhibitor. As shown in Fig. 4*C*, the effect of Mel-18 antisense on cyclin D1 expression and $p27^{Kip1}$ phosphorylation was abrogated when cells were treated with LY294002 (*lane 3* versus *lane 2*), but not with PD98059 (*lane 4* versus *lane 2*; $P = 0.008$ and $P = 0.009$, respectively, Student's *t* test). Interestingly, endogenous expression of Mel-18 was up-regulated by LY294002 treatment (*lane 3* versus *lane 2*). Likewise, the phosphatidylinositol 3-kinase inhibitor wortmannin also increased Mel-18 expression (data not shown). Collectively, these results show that the changes seen in cyclin D1 expression and $p27^{Kip1}$ phosphorylation by Mel-18 are mediated by the Akt signaling pathway but not by the Erk pathway.

Mel-18 blocks Akt-mediated cytoplasmic localization of $p27^{Kip1}$. Direct phosphorylation of $p27^{Kip1}$ at Thr^{157} by Akt is implicated in inhibition of its nuclear import (20–22). Because we found that Mel-18 down-regulated $p27^{Kip1}$ phosphorylation at Thr^{157} (Fig. 3*A*), the effect of Mel-18 on subcellular localization of $p27^{Kip1}$ was examined. SK-BR-3 cells were infected with retroviral vector encoding each construct (control, Mel-18, $p27^{Kip1}\Delta$NLS mutant) or treated with 40 μmol/L LY294002. The overexpression of Mel-18 and $p27^{Kip1}\Delta$NLS mutant and the Akt inhibition effect of LY294002 were confirmed by Western blot analysis (Fig. 5*A*). We found that cytoplasmic $p27^{Kip1}$ expression was reduced and nuclear $p27^{Kip1}$ expression was enhanced by Mel-18 as determined by cytoplasmic and nuclear fractionations and immunoblotting (Fig. 5*B*). To confirm these data, we also carried out immunofluorescence staining in these cells. Consistent with the above result, cytoplasmic $p27^{Kip1}$ was reduced in Mel-18–overexpressing SK-BR-3 cells ($P < 0.05$, Student's *t* test; Fig. 5*C*). Therefore, these results suggest that Mel-18 affects Akt-mediated $p27^{Kip1}$ localization in human breast cancer.

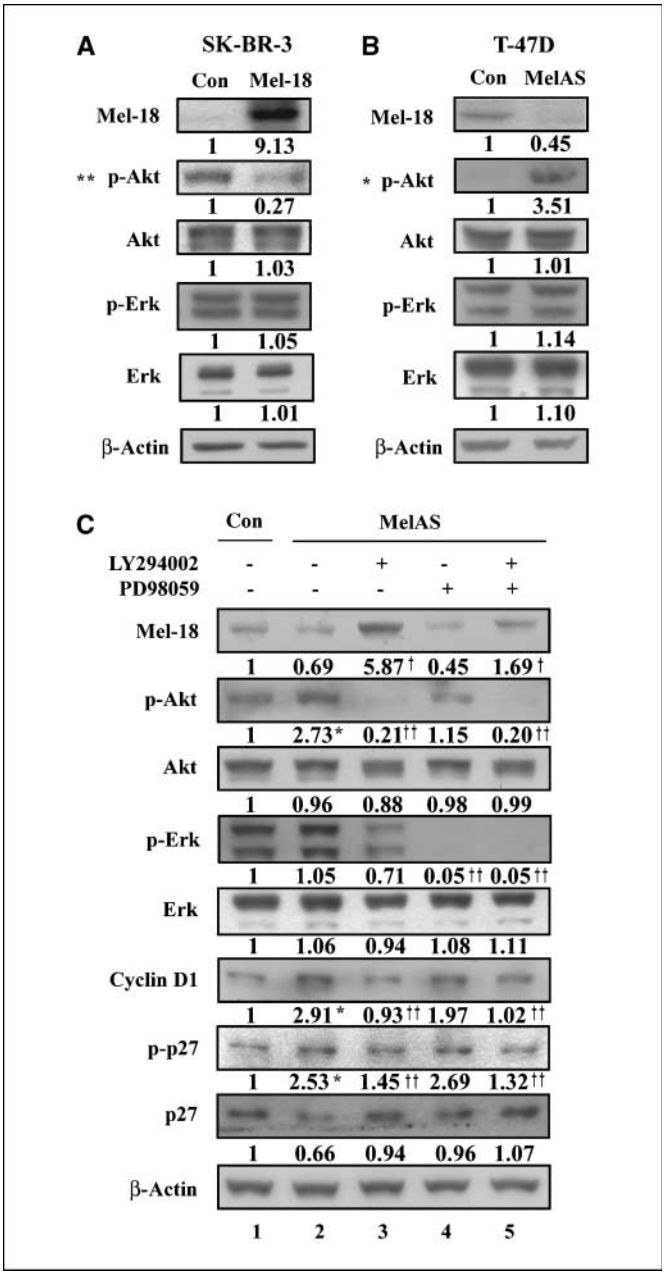

Figure 4. Mel-18 regulates cyclin D1 expression and $p27^{Kip1}$ phosphorylation via the Akt signaling pathway but not the Erk pathway. *A* and *B*, transiently transduced SK-BR-3 and T-47D, prepared as in Fig. 3, were subjected to immunoblotting to examine the changes in Akt and Erk expression and phosphorylation. The Western blot densities were measured and statistically analyzed with Student's *t* test. * and **, $P < 0.05$, statistically significant increase and decrease, respectively. *C*, four days after release from synchronization, T-47D cells were treated with 40 μmol/L LY294002 and/or 50 μmol/L PD98059 for 24 h, and subjected to immunoblotting with antibodies as indicated. Representative of three independent experiments with similar results. *, $P < 0.05$, statistically significant increase compared with *lane 1*; † and ††, $P < 0.05$, statistically significant increase and decrease compared with *lane 2*, respectively.

Mel-18 inhibits the Akt-mediated Wnt signaling pathway. Because cyclin D1 expression was affected by Mel-18 at both protein and transcript levels (Fig. 3*B* and *C*) and the Akt signaling pathway was implicated (Fig. 4*C*), we tested whether the Akt-mediated Wnt signaling pathway was involved in the regulation of cyclin D1 expression. In Mel-18–infected SK-BR-3 cells, GSK-3β

phosphorylation at Ser^9 was diminished whereas total GSK-3β expression remained unchanged as determined by immunoblotting (Fig. 6*A, left*). Likewise, enhanced GSK-3β phosphorylation at Ser^9 was seen in Mel-18 antisense–infected T-47D cells (Fig. 6*A, right*). However, total β-catenin expression remained unchanged in both cell lines (Fig. 6*A*). Because inhibition of GSK-3β phosphorylation implicates reduced nuclear β-catenin (15), we next investigated the subcellular localization of β-catenin on Mel-18 overexpression in SK-BR-3 cells. As shown in Fig. 6*B*, cytoplasmic β-catenin expression was increased and nuclear β-catenin expression was decreased by Mel-18 overexpression as assessed by biochemical fractionation of nuclear and cytoplasmic proteins and immunoblotting. Consistent with this result, enhanced localization of β-catenin in the cytoplasm was seen in Mel-18–overexpressing cells as determined by immunofluorescence staining ($P < 0.05$, Student's *t* test; Fig. 6*C*). Furthermore, the reduction of nuclear β-catenin by Mel-18 in SK-BR-3 cells also reduced TCF/LEF promoter activity, as assessed by reporter assays with β-catenin–dependent TCF/LEF promoter (TOP-FLASH) and its mutant (FOP-FLASH; $P = 0.01$, Student's *t* test; Fig. 6*D*). Taken together, Mel-18 effect on cyclin D1 transcription is mediated by the Akt-dependent canonical Wnt signaling pathway.

Discussion

In this study, we report that Mel-18 regulates cell cycle progression by down-regulation of the Akt signaling pathway in human breast cancer. In primary breast tumors, the expression of Mel-18 was inversely correlated with phosphorylation of Akt at Ser^{473}, which is phosphorylated in activated Akt. Mel-18 expression was also correlated with the percentage of the G_1 phase population by regulating the activities of Cdk4 and Cdk2 in T-47D and SK-BR-3 breast cancer cell lines. Those Cdk activities were affected by changes in cyclin D1 expression and $p27^{Kip1}$ phosphorylation, but not in *INK4a/ARF* gene family. Cyclin D1 expression was regulated by the Akt-mediated Wnt signaling pathway, and cytoplasmic

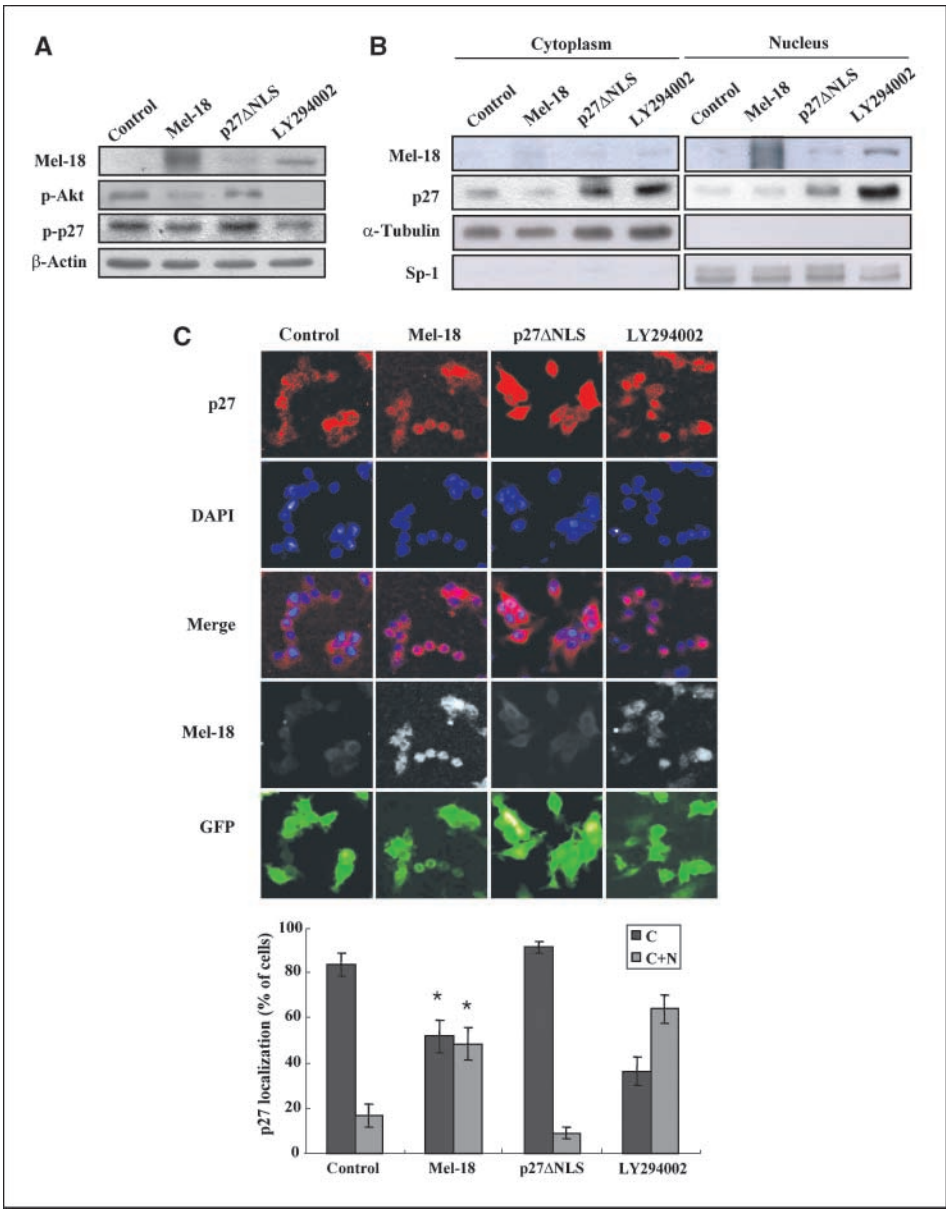

Figure 5. Inhibition of cytoplasmic localization of $p27^{Kip1}$ by Mel-18 overexpression in SK-BR-3 cells. SK-BR-3 cells were transiently infected with retroviral empty vector (*Control*), Mel-18, and $p27^{Kip1}$ΔNLS (*p27ΔNLS*), as in Fig. 3, or treated with 40 μmol/L LY294002 for 24 h, as in Fig. 4*C*. *A,* each cell lysate was subjected to immunoblotting with indicated antibodies. *B,* cells were fractionated and the amounts of nuclear and cytoplasmic $p27^{Kip1}$ were estimated by immunoblotting. $p27^{Kip1}$Δ NLS mutant construct and LY294002 treatment were used as positive controls for cytoplasmic $p27^{Kip1}$ and nuclear $p27^{Kip1}$, respectively. α-Tubulin and Sp1 were tested as controls of cytoplasmic and nuclear fractionations, respectively. *C,* cells were costained with anti-$p27^{Kip1}$ antibody coupled with Cy5-conjugated antimouse immunoglobulin (IgG; *red*) and anti–Mel-18 antibody coupled with phycoerythrin-conjugated antirabbit IgG (*white*). The efficiency of retroviral infection was determined by observation of green fluorescent protein (*GFP*) expression (*green*). To visualize the nucleus, DAPI staining was also done (*blue*). The ratio of the cytoplasmic and nuclear $p27^{Kip1}$ expression was measured by counting 1,000 cells each in three independent experiments and the result was shown as percentage of total cells counted ± SD (*bottom*). *, $P < 0.05$ (Student's *t* test).

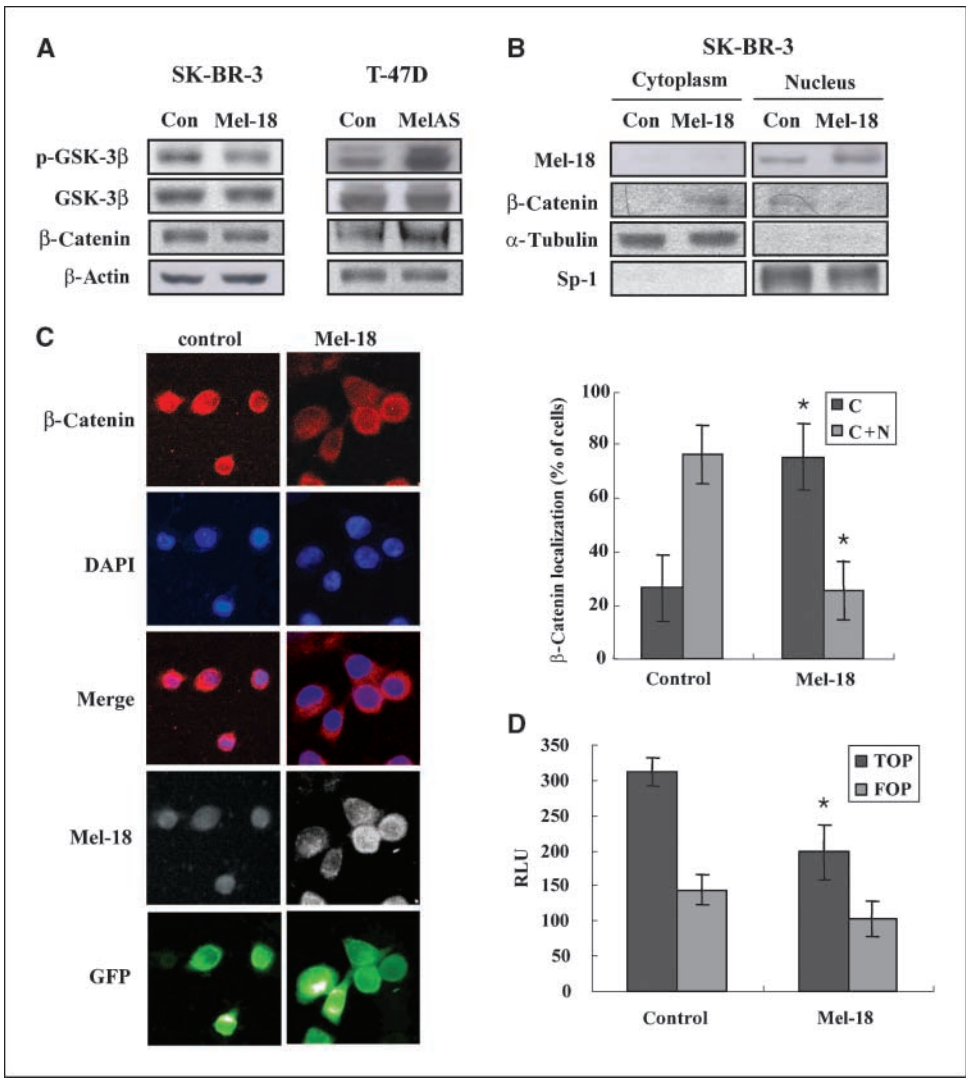

Figure 6. Mel-18 inhibits the Akt-mediated canonical Wnt pathway. *A,* transiently transduced SK-BR-3 and T-47D cells, as in Fig. 3, were subjected to immunoblotting with indicated antibodies. *B,* Mel-18–infected SK-BR-3 cells were fractionated and the amounts of nuclear and cytoplasmic β-catenin expression were estimated by Western blot analysis. α-Tubulin and Sp1 were tested as controls of cytoplasmic and nuclear fractions, respectively. *C,* cells were stained with β-catenin antibody coupled with Cy5-conjugated antimouse IgG (*red*) and Mel-18 antibody as in Fig. 5*C*. To observe the nucleus, cells were also subjected to DAPI staining (*blue*; *left*). *Right,* ratio of the cytoplasmic and nuclear β-catenin expression quantified by counting 1,000 cells each in three independent experiments and shown as percentage of total cells counted; *bars,* SD. *D,* the effect of Mel-18 overexpression on TCF/LEF promoter activity was determined by reporter assay as described in Materials and Methods. *Columns,* mean of triplicate transfections; *bars,* SD. *TOP,* reporter assay with TOP-FLASH construct; *FOP,* reporter assay with FOP-FLASH construct; *RLU,* relative light units. *, $P < 0.05$ (Student's *t* test).

retention of $p27^{Kip1}$ was reduced by inhibition of Akt-dependent phosphorylation at Thr^{157}. Taken together, we show a linear relationship between Mel-18, Akt, and G_1 phase regulators.

The oncogenic properties of several PcG proteins such as Bmi-1, RNF2, and CBX7 are, at least in part, attributed to repression of *Cdkn2a* locus, the tumor-suppressive locus encoding INK4a and ARF proteins (2). They can control G_1-S transition in cell cycle progression and senescence via targeting *INK4a/ARF* locus (29, 34, 35). Mel-18 has also been reported as an inhibitor of *INK4a/ARF* genes (29, 30). However, a recent report shows that Mel-18 accelerates cellular senescence through down-regulation of Bmi-1 and up-regulation of its target genes, $p16^{INK4a}$ and $p14^{ARF}$, in human fibroblast (31). As we previously showed that Mel-18 interacts with cyclin D2 and inhibits the proliferative activity of cyclin D2 in breast cancer (11), we have further examined the role of Mel-18 in cell cycle progression. Here, we suggest that Mel-18 negatively regulates cell cycle of human breast cancer in a *INK4a/ARF*–independent manner. The *INK4a/ARF* locus is frequently silenced in human primary breast tumors (36–38). The expression levels of these genes were also very weak or undetectable in human breast cancer cell lines including T-47D (data not shown). Although their expression patterns were undetectable or remained unchanged, Mel-18 could affect the G_1-S transition through changes in Cdk4 and Cdk2 activities via regulation of other G_1 phase regulators, particularly cyclin D1 and $p27^{Kip1}$ (Fig. 3).

At the molecular level, we show here that Mel-18–induced G_1 arrest via changes in cyclin D1 expression and $p27^{Kip1}$ phosphorylation at Thr^{157} is mediated by Akt signaling. We found that Mel-18 down-regulated cyclin D1 transcription via the Akt-mediated Wnt signaling pathway (Figs. 3*B–C* and 6). Moreover, reduced $p27^{Kip1}$ phosphorylation at Thr^{157} by Mel-18 led to inhibition of Akt-mediated cytoplasmic localization of $p27^{Kip1}$ (Figs. 3*B–C* and 5). These changes in Akt-mediated G_1 regulators may explain how Mel-18 regulated cell cycle progression of breast cancer cells, which have hypermethylated *INK4a/ARF* genes, in an *INK4a/ARF*–independent manner. Recently, Guo et al. (12) reported the novel relationship between Mel-18 and Akt. Although our results partially overlap with their results in showing the relationship between Mel-18 and Akt, the significance of this study is that our focus is different from them. They suggest that Bmi-1 enhances Akt activity and Mel-18–mediated Bmi-1 down-regulation leads to inhibition its activity. Although, we did not look into the role of Bmi-1 in our system, we also show the relationship between Mel-18 expression and Akt activation both *in vitro* and *in vivo*. We found an inverse correlation between Mel-18 expression and Akt phosphorylation at Ser^{473} in human primary breast cancer (Fig. 1). This result is

consistent with two previous reports, which showed decreased Mel-18 mRNA in human breast cancer cell lines (39) and low expression of Mel-18 in primary breast cancer (12). Although Guo et al. (12) first reported the relationship between Mel-18 and Akt activity, they have seen it in the *in vitro* cultured cells. We also show Mel-18–mediated Akt activity in other two breast cancer cell lines, SK-BR-3 and T-47D, by either overexpression or knockdown of Mel-18. Taken together, we established a linear relationship between Mel-18→Akt→G_1 phase regulators, which is compatible with the Mel-18→Bmi-1→Akt model of Guo et al., yet an extension of their model. Moreover, our results may be another evidence of the tumor-suppressive effect of Mel-18 in human breast cancer.

Although we observed Mel-18–mediated Akt signaling, the exact regulatory mechanism of Akt activity by Mel-18 remains to be elucidated. Because Mel-18 is reported as a transcriptional repressor by binding of specific DNA sequence (10), and Mel-18 is dominantly expressed in the nucleus (11) whereas Akt is expressed in the cytosol, Mel-18 may regulate Akt activity indirectly by repressing transcription of certain positive regulators of Akt, such as phosphatidylinositol 3-kinase or phosphoinositide-dependent kinases, by binding to its target sequences rather than by directly binding to Akt and inhibiting its activity.

Collectively, we propose that Mel-18 acts as a negative regulator of cell cycle in G_1-S transition through regulation of Akt-mediated cyclin D1 expression and $p27^{Kip1}$ phosphorylation at Thr^{157} in *INK4a/ARF*–silenced human breast cancer, and it may suggest the greater possibility of tumor-suppressive activity of Mel-18 in these cancer cells.

Acknowledgments

Received 7/7/2007; revised 12/23/2007; accepted 2/28/2008.

Grant support: Korea Science and Engineering Foundation grant 2007-04369 funded by the Korean government (Ministry of Science and Technology).

The costs of publication of this article were defrayed in part by the payment of page charges. This article must therefore be hereby marked *advertisement* in accordance with 18 U.S.C. Section 1734 solely to indicate this fact.

We thank Dr. S.J. Hwang (Hanyang University, Seoul, Korea) for the technical support for immunofluorescence staining and Dr. H.K. Chung (Hanyang University, Seoul, Korea) for critical comments and reading of the manuscript.

References

1. Jacobs JJ, van Lohuizen M. Cellular memory of transcriptional states by Polycomb-group proteins. Semin Cell Dev Biol 1999;10:227–35.
2. Sparmann A, van Lohuizen M. Polycomb silencers control cell fate, development and cancer. Nat Rev Cancer 2006;6:846–56.
3. Gil J, Bernard D, Peters G. Role of polycomb group proteins in stem cell self-renewal and cancer. DNA Cell Biol 2005;24:117–25.
4. Wiederschain D, Chen L, Johnson B, et al. Contribution of polycomb homologues Bmi-1 and Mel-18 to medulloblastoma pathogenesis. Mol Cell Biol 2007;27:4968–79.
5. Vonlanthen S, Heighway J, Altermatt HJ, et al. The bmi-1 oncoprotein is differentially expressed in non-small cell lung cancer and correlates with INK4A-ARF locus expression. Br J Cancer 2001;84:1372–6.
6. Dimri GP, Martinez JL, Jacobs JJ, et al. The Bmi-1 oncogene induces telomerase activity and immortalizes human mammary epithelial cells. Cancer Res 2002;62:4736–45.
7. Leung C, Lingbeek M, Shakhova O, et al. Bmi1 is essential for cerebellar development and is overexpressed in human medulloblastomas. Nature 2004;428:337–41.
8. Tagawa M, Sakamoto T, Shigemoto K, et al. Expression of novel DNA-binding protein with zinc finger structure in various tumor cells. J Biol Chem 1990;265:20021–6.
9. Dukers DF, van Galen JC, Giroth C, et al. Unique polycomb gene expression pattern in Hodgkin's lymphoma and Hodgkin's lymphoma-derived cell lines. Am J Pathol 2004;164:873–81.
10. Kanno M, Hasegawa M, Ishida A, Isono K, Taniguchi M. mel-18, a Polycomb group-related mammalian gene, encodes a transcriptional negative regulator with tumor suppressive activity. EMBO J 1995;14:5672–8.
11. Chun T, Rho SB, Byun HJ, Lee JY, Kong G. The polycomb group gene product Mel-18 interacts with cyclin D2 and modulates its activity. FEBS Lett 2005;579:5275–80.
12. Guo WJ, Zeng MS, Yadav A, et al. Mel-18 acts as a tumor suppressor by repressing Bmi-1 expression and down-regulating Akt activity in breast cancer cells. Cancer Res 2007;67:5083–9.
13. Vivanco I, Sawyers CL. The phosphatidylinositol 3-Kinase AKT pathway in human cancer. Nat Rev Cancer 2002;2:489–501.
14. Cross DA, Alessi DR, Cohen P, Andjelkovich M, Hemmings BA. Inhibition of glycogen synthase kinase-3 by insulin mediated by protein kinase B. Nature 1995;378:785–9.
15. Sharma M, Chuang WW, Sun Z. Phosphatidylinositol 3-kinase/Akt stimulates androgen pathway through GSK3β inhibition and nuclear β-catenin accumulation. J Biol Chem 2002;277:30935–41.
16. Medema RH, Kops GJ, Bos JL, Burgering BM. AFX-like Forkhead transcription factors mediate cell-cycle regulation by Ras and PKB through p27kip1. Nature 2000;404:782–7.
17. Stahl M, Dijkers PF, Kops GJ, et al. The forkhead transcription factor FoxO regulates transcription of p27Kip1 and Bim in response to IL-2. J Immunol 2002;168:5024–31.
18. Schmidt M, Fernandez de Mattos S, van der Horst A, et al. Cell cycle inhibition by FoxO forkhead transcription factors involves down-regulation of cyclin D. Mol Cell Biol 2002;22:7842–52.
19. Diehl JA, Cheng M, Roussel MF, Sherr CJ. Glycogen synthase kinase-3β regulates cyclin D1 proteolysis and subcellular localization. Genes Dev 1998;12:3499–511.
20. Liang J, Zubovitz J, Petrocelli T, et al. PKB/Akt phosphorylates p27, impairs nuclear import of p27 and opposes p27-mediated G_1 arrest. Nat Med 2002;8:1153–60.
21. Shin I, Yakes FM, Rojo F, et al. PKB/Akt mediates cell-cycle progression by phosphorylation of p27(Kip1) at threonine 157 and modulation of its cellular localization. Nat Med 2002;8:1145–52.
22. Viglietto G, Motti ML, Bruni P, et al. Cytoplasmic relocalization and inhibition of the cyclin-dependent kinase inhibitor p27(Kip1) by PKB/Akt-mediated phosphorylation in breast cancer. Nat Med 2002;8:1136–44.
23. Zhou BP, Liao Y, Xia W, Spohn B, Lee MH, Hung MC. Cytoplasmic localization of p21Cip1/WAF1 by Akt-induced phosphorylation in HER-2/neu-overexpressing cells. Nat Cell Biol 2001;3:245–52.
24. Wu FY, Wang SE, Sanders ME, et al. Reduction of cytosolic p27(Kip1) inhibits cancer cell motility, survival, and tumorigenicity. Cancer Res 2006;66:2162–72.
25. Yoo YG, Oh SH, Park ES, et al. Hepatitis B virus X protein enhances transcriptional activity of hypoxia-inducible factor-1α through activation of mitogen-activated protein kinase pathway. J Biol Chem 2003;278:39076–84.
26. Chung H, Jung JY, Cho SD, et al. The antitumor effect of LJ-529, a novel agonist to A3 adenosine receptor, in both estrogen receptor-positive and estrogen receptor-negative human breast cancers. Mol Cancer Ther 2006;5:685–92.
27. van de Wetering M, Cavallo R, Dooijes D, et al. Armadillo coactivates transcription driven by the product of the *Drosophila* segment polarity gene dTCF. Cell 1997;88:789–99.
28. Altomare DA, Testa JR. Perturbations of the AKT signaling pathway in human cancer. Oncogene 2005;24:7455–64.
29. Jacobs JJ, Kieboom K, Marino S, DePinho RA, van Lohuizen M. The oncogene and Polycomb-group gene bmi-1 regulates cell proliferation and senescence through the ink4a locus. Nature 1999;397:164–8.
30. Kranc KR, Bamforth SD, Braganca J, Norbury C, van Lohuizen M, Bhattacharya S. Transcriptional coactivator Cited2 induces Bmi1 and Mel18 and controls fibroblast proliferation via Ink4a/ARF. Mol Cell Biol 2003;23:7658–66.
31. Guo WJ, Datta S, Band V, Dimri GP. Mel-18, a polycomb group protein regulates cell proliferation and senescence via transcriptional repression of Bmi-1 and c-Myc oncoproteins. Mol Biol Cell 2007;18:536–46.
32. Liang J, Slingerland JM. Multiple roles of the PI3K/PKB (Akt) pathway in cell cycle progression. Cell Cycle 2003;2:339–45.
33. Lenferink AE, Busse D, Flanagan WM, Yakes FM, Arteaga CL. ErbB2/neu kinase modulates cellular p27(Kip1) and cyclin D1 through multiple signaling pathways. Cancer Res 2001;61:6583–91.
34. Bernard D, Martinez-Leal JF, Rizzo S, et al. CBX7 controls the growth of normal and tumor-derived prostate cells by repressing the Ink4a/Arf locus. Oncogene 2005;24:5543–51.
35. Voncken JW, Roelen BA, Roefs M, et al. Rnf2 (Ring1b) deficiency causes gastrulation arrest and cell cycle inhibition. Proc Natl Acad Sci U S A 2003;100:2468–73.
36. Dominguez G, Silva J, Garcia JM, et al. Prevalence of aberrant methylation of p14ARF over p16INK4a in some human primary tumors. Mutat Res 2003;530:9–17.
37. Brenner AJ, Paladugu A, Wang H, Olopade OI, Dreyling MH, Aldaz CM. Preferential loss of expression of p16(INK4a) rather than p19(ARF) in breast cancer. Clin Cancer Res 1996;2:1993–8.
38. Sharma G, Mirza S, Prasad CP, Srivastava A, Gupta SD, Ralhan R. Promoter hypermethylation of p16INK4A, p14ARF, cyclinD2 and Slit2 in serum and tumor DNA from breast cancer patients. Life Sci 2007;80:1873–81.
39. Matsuo F, Yano K, Saito H, et al. Mutation analysis of the mel-18 gene that shows decreased expression in human breast cancer cell lines. Breast Cancer 2002;9:33–8.